Enrichment differentiation of human induced pluripotent stem cells into sinoatrial node-like cells by combined modulation of BMP, FGF and RA signaling pathways

Feng Liu
Southwest Medical university
YiBing Fang
Southwest Medical University
XiaoJie Hou
Southwest Medical University
Ying Yan
Southwest Medical University
HaiYing Xiao
Southwest Medical University
DongChuan Zuo
Southwest Medical University
Jing Wen
Southwest Medical University
LinLi Wang
Guangzhou Biocare Institute of Cancer
XiTong Dang
SouthWest Medical University
Rui Zhou (zhouhuaxizhu@swmu.edu.cn)
Southwest Medical University
Bin Liao
Southwest Medical University

Research

Keywords: human induced pluripotent stem cell (hiPSC), sinus atrial node like cells (SANLC), bone morphogenetic protein (BMP) signaling, fibroblast growth factor (FGF) signaling, retinoic acid (RA) signaling

Posted Date: February 18th, 2020

DOI: https://doi.org/10.21203/rs.2.23881/v1

Version of Record: A version of this preprint was published on July 16th, 2020. See the published version at https://doi.org/10.1186/s13287-020-01794-5.

Abstract

Background : Biological pacemakers derived from pluripotent stem cell (PSC) have been considered as a potential therapeutic surrogate for sick sinus syndrome. So it's essential to develop high efficient strategies for enrichment of sinoatrial node-like cells (SANLC) as seed cells for biological pacemakers. It has reported that BMP, FGF and RA signaling pathways were involved specification of different cardiomyocyte subtypes, pacemaker, ventricle, and atria cells.

Methods : During the differentiation process from human induced pluripotent stem cell (hiPSC) to cardiomyocyte through small molecule based temporal modulation of the Wnt signaling pathway, signaling of BMP, FGF and RA was manipulated at cardiac mesoderm stage. The methods of qRT-PCR, immunofluorescence, flow cytometry and whole cell patch clamp were used to identify the SANLC.

Results : qRT-PCR results showed that manipulating each one of BMP, FGF and RA signaling was effective for the upregulation of SANLC markers. Moreover, combined modulation of such three pathways displayed the best efficiency for the expression of SANLC markers, which was further confirmed at protein level using immunofluorescence, flow cytometry. Finally, the electrophysiological characteristics of induced SANLC were verified by patch clamp method.

Conclusion : An efficient transgene-independent differentiation protocol for generating SANLC from hPSC was developed, in which combined modulating BMP, FGF and RA signaling at cardiac mesoderm stage generates SANLC at high efficiency. It may serve as a potential approach for biological pacemaker construction.

Introduction

"Sick sinus syndrome" (SSS) is a group of heart arrhythmia caused by perturbed function of the sinus node that is composed of cardiac pacemaker cells. They include pathological and/or symptomatic sinus bradycardia, sinoatrial (SA) block and tachycardia-bradycardia syndrome. Although implantation of electronic pacemaker has been one of the most effective treatments at present,it is associated with significant risks of infection, hemorrhage, and lead dislodging. Moreover, limited battery life and lack of autonomic neurohumoral responses further limit its usage [1, 2]. Therefore, the "biological pacemaker" derived from human pluripotent stem cells (hPSC) may provide a promising alternative treatment.

Cardiomyocytes differentiation from hPSC is recognized as a powerful model to simulate the human embryonic heart development in vivo and is a promising source of cardiomyocytes for regenerative medicine. The embryonic heart development experiences several spatial-temporal stages from primitive streak to cardiac crescent and then to primitive heart tube, and the latter forms distinct anterior and posterior poles containing different mesodermal progenitors that give rise to different cardiomyocyte subtypes including ventricular, atrial and SAN-like cardiomyocytes (SANLC) [3–5]. Up to now, most protocols were designed to generate heterogenous ventricular cardiomyocytes with a very small percentage of atrial and SANLC [6, 7]. Analyses of early developmental stages revealed that ventricular,

atrial and SAN-like cardiomyocytes were derived from different mesoderm cell populations that could be distinguished based on their expression of CD235a [8, 9], RALDH2 [8] and TBX18 [10–12], respectively. In addition, it was found that different signaling pathways were involved different cardiomyocyte subtypes specification. For example, retinoic acid (RA) signaling at the mesoderm stage is required for atrial specification [8], while ventricular specification is highly dependent on the fibroblast growth factor (FGF) signaling [13–16]. A recent study showed that bone morphogenetic protein (BMP) signaling plays an important role in the specification of mesoderm progenitors into SANLC [17, 18]. These early discoveries suggest that hiPSC-induced cardiomyocytes can be directed to differentiate into SAN-like cardiomyocytes at cardiac mesoderm stage by activation of signaling pathways leading to SAN-like, and simultaneous inhibition of signaling pathways leading to ventricular and atrial cardiomyocytes.

Here, we have established a developmental-biology-based approach to enrich SANLC from hiPSC. We find that activation of BMP and simultaneous inhibition of RA and FGF signaling pathways during cardiac mesoderm stage of hiPSC differentiation can significantly enrich SAN-like cardiomyocytes, which will facilitate the study of human SAN development provide a rich source of cells for the development of biological pacemaker.

Materials And Methods

Materials

The LHpb-YaabC3 hiPSC was obtained from OSINGLAY BIO (China), and BJ human foreskin fibroblast cell line was purchased from American Type Culture Collection (ATCC). Cell culture media RPMI/1640 (11875093, USA) and DMEM/F12 media (11320082, USA) were from Thermo Fisher Scientific, and medium for hiPSC BioCISO was from BIOCARE Biotech (BC-PM0001, China). GSK3 inhibitor CHIR99021 was from Sigma (S1263, USA). FGF inhibitor PD (3044, UK), Wnt inhibitor IWP2 (3533, UK) and ROCK inhibitor Y27632 (1254, UK) were obtained from Tocris Bioscience. BMP activator BMP4 (120-05ET, USA) and RA inhibitor BMS were from Sigma (SML1149, USA). B-27 supplement with (17504-044, USA) or without insulin was purchased from Thermo Fisher Scientific. Matrigel was bought from Corning (354277, UK). TRIzol Reagent was bought from Thermo Fisher Scientific (15596026, USA). Real-time PCR reagents were purchased from Qiagen (208056, Germany). All primers/oligos were synthesized by Shenggong Biotech (China) and listed in supplemental Table 1. All other reagents, unless specified otherwise, were products of Sigma.

Cardiomyocytes Differentiation From hiPSC

Cardiomyocyte differentiation was performed in a growth factor and serum-free system by temporal modulation of the canonical Wnt signaling pathway with GSK3 inhibitor (Gi) and Wnt inhibitor (Wi), known as the GiWi protocol [19]. Briefly, 80–90% confluent hiPSC was harvested using 0.5 mM EDTA, and resuspended with hiPSC maintaining medium at 0.5×10^5 cells per ml. Two ml of the cell suspension was seeded per well in a 12-well matrigel-coated plate with 2 ml of hiPSC at day-4. At day 0 the medium was refreshed with RPMI/B-27 containing CHIR99021 (10 μM, GSK3 inhibitor) without insulin and continued

to incubate for 24 h. The medium was replaced with RPMI/B-27 without insulin for another 48 h. On day 3 of the differentiation (72 h after addition of CHIR99021), medium was refreshed with RPMI/B-27 containing IWP2 (5 μM, Wnt inhibitor) without insulin for 48 h, followed by RPMI/B-27 without insulin from day 5 to 7. From day 7, the medium was refreshed with RPMI/B-27 containing insulin every 3 days. The beating cardiomyocytes can be seen as early as on day 8.

RNA Isolation And qPCR

Total RNA was isolated using Trizol method (15596026, USA). One μg of total RNA was reversely transcribed in a total volume of 10 μl with ReverTra Ace qPCR RT Master Mix kit (FSQ-201, TOYOBO, Japan) following manufacturer's instructions. The cDNA was diluted 3 times, and 1 μl was used for real-time PCR in a 20 μl reaction using SYBR Green Real Time PCR Mix (204143, Qiagen, Germany). The PCR conditions were 95 °C for 2 min, followed by 40 cycles of 95 °C for 20" and 60 °C for 15". All primers were listed in supplement table 1. The expression of target gene was normalized to that of GAPDH and calculated using $2^{-\Delta\Delta Ct}$ method.

Immunofluorescence

Single hiPSC cells and induced cardiomyocytes were seeded in a μ-Slide 8 well (80827, ibidi) coated with Matrigel at the density of 2×10^4 per well for 48 h. Cells were fixed with 4% (w/v) Paraformaldehyde (PFA) for 15 min at room temperature, permeabilized, and incubated with the following primary antibodies: anti-OCT4 antibody (#2750, Cell Signaling Technology, USA), anti-NANOG antibody (#3580, Cell Signaling Technology, USA), anti-SSEA4 antibody (#4755, Cell Signaling Technology, USA), anti-TRA-1-60 antibody (#4746, Cell Signaling Technology, USA), anti-Ki67 antibody (ab15580, abcam, USA), anti-NKX2.5 antibody (ab91196, abcam, USA), anti-cTNT antibody (MS-295-P1, Thermo Fisher Scientific, USA), anti-α-actinin antibody (A7811, Sigma, USA), anti-SHOX2 antibody (ab55740, abcam, USA), anti-TBX18 antibody (ab115262, abcam, USA), and anti-TBX3 antibody (ab154828, abcam, USA), followed by the following species-specific fluorence-conjugated secondary antibodies: alexa fluor 488 labeled goat anti-rabbit IgG (A-11008, Invitrogen, USA), alexa fluor 488 labeled goat anti-mouse IgG (A-11001, Invitrogen, USA), alexa fluor 594 labeled goat anti-rabbit IgG (R37177, Invitrogen, USA) and alexa fluor 594 labeled goat anti-mouse IgG (A-11005, Invitrogen, USA). The cells were then counterstained using 0.5 μg/ml of DAPI (4083, Cell Signaling Technology, USA) for 15 min at room temperature. After rinsing with PBS, the chambers were mounted and visualized under fluorescence microscopy (IX83, Olympus, Japan).

Flow Cytometry

The induced cardiomyocytes in 12-well plate were digested with 0.25% trypsin with 0.5 mM EDTA into single cell suspension and washed with PBS. Cells were fixed with 4% formaldehyde for 10 min at room temperature and chilled on ice for 1 min. Permeablization was performed by adding one tenth of ice-cold 100% methanol slowly to the pre-chilled cells and continue to incubate on ice for 30 min. Cells were then blocked with blocking buffer (0.5% BSA in PBS) for 10 min, incubated with the following primary antibodies, anti-cTNT antibody (MS-295-P1, Thermo Fisher Scientific), anti-NKX2-5 antibody (ab91196,

abcam, USA), and anti-SHOX2 antibody (ab55740, abcam, USA) for 1 h at room temperature, washed with PBS, and followed by incubation with the corresponding species-specific fluorence-conjugated secondary antibodies, alexa fluor 488 labeled goat anti-mouse IgG (A-11029, Invitrogen),alexa fluor 488 labeled goat anti-rabbit IgG (A-11034, Invitrogen), alexa fluor 647 labeled goat anti-mouse IgG (A-21235, Invitrogen), and alexa fluor 647 labeled goat anti-rabbit IgG (A-32733, Invitrogen) for 30 min at room temperature. Cells were analyzed using Flow cytometry machine (BD FACS Verse, BD Bioscience, USA) according to the manufacturer's protocol.

Action Potential (AP) Recording

AP recording was performed following El-Battrawy I's protocol with some modifications [20]. Briefly, on 60 days after cardiomyocytes differentiation, induced cardiomyocytes were dissociated into single cell suspension by 30 min's type collagenase (2 mg/ml) followed by 3 min's Trypsin (0.25%) without EDTA. 1×10^4 cells were seeded into a 3.5 cm dish containing a lysine-treated glass coverslip and incubated for 3 days. AP was recorded using the whole cell patch clamp electrophysiology method. Briefly, the adherent cells on the coverslip were placed in the recording chamber and perfused with bath solution containing 140 mM NaCl, 1 mM $MgCl_2$, 5 mM KCl, 1.8 mM $CaCl_2$, 5 mM 4-(2-hydroxyethyl)-1-piperazineethanesulfonic acid (HEPES) and 10 mM glucose, (The pH was adjusted to 7.40, and the osmolality to 301 ± 3 mOsm, respectively). The patch pipettes were pulled from borosilicate glass capillaries (Drummond, USA) by a horizontal puller (NARISHIGE, Japan) and had resistances of 1.5–3 MΩ. Pipette solution consisted of 110 mM K-gluconate, 20 mM KCl, 1 mM $CaCl_2$, 1 mM $MgCl_2$, 10 mM HEPES, 5 mM ethylene glycol tetraacetic acidpotassium chloride (EGTA-KOH), 5 mM ATP-Mg^{2+}, 5 mM Na-phosphocreatine. The pH was adjusted to 7.2 by KOH and the osmolality to 290 ± 3 mOsm. A Multiclamp 700B amplifier was used to record APs, and data were analyzed using a custom software.

Statistical analysis

Experimental data are presented as "mean ± SD" with at least three repeats. Between groups comparisons were performed using one-way analysis of variance (one-way ANOVA), with $p < 0.05$ was considered statistically significant.

Results

Characterization of hiPSC

hiPSC was purchased from OSINGLAY BIO company. To confirm the authenticity of the hiPSC, the molecular signature of hiPSC was validated by both qRT-PCR and Immunofluorescence (IF). The qRT-PCR results showed that the hiPSC expresses stem cell-specific markers, OCT3/4, SOX2 and NANOG that are non-detectable in the human terminal differentiated fibroblast cells (Bj), and the expression levels of the three stem cell-specific markers are relatively high, as judged by their similar cycle threshold (Ct) values that are comparable to that of the house-keeping gene, GAPDH (Fig. 1A). The IF results showed that the hiPSC is proliferative (Ki67 positive) (Fig. 1B) and heavily stained for NANOG, OCT4, SSEA4 and TRA-1-

60, which are localized in nuclei (for NANOG and OCT4 and plasma membrane (for SSEA4 and TRA-1-60) respectively (Fig. 1C-F). Which was further confirmed using flow cytometry analysis (Fig. 1G, H). These results demonstrate that the hiPSC possesses their pluripotency and self-renewal capability.

Identification Of hiPSC Induced Cardiomyocytes

Cardiomyocytes were induced by the widely used GiWi protocol originally proposed by Lian, et al [19], where the induction process was temporally initiated using GSK3 inhibitor (Gi) and followed by temporal inhibition of the Wnt signaling pathway using Wnt inhibitor (Wi). To optimize the induction protocol, different concentrations of the Gi, CHIR were added on day 0 of the differentiation and continued to incubate for 24 h, and the markers of mesoendoderm (BRACHYURY) and cardiac mesoderm (MESP1) were evaluated on day 1 and day 3 using qRT-PCR. CHIR dose-dependently increased the expression of both BRACHYURY (Fig. 2A) and MESP1 (Fig. 2B) on day 1, with CHIR at 10 μM reached the highest level. Similar dose-response curves were observed on day 3 for both markers, however the overall levels of BRACHYURY (Fig. 2A) were significantly decreased, whereas the levels of MESP1 (Fig. 2B) were significantly increased, at different concentrations of CHIR compared to those levels on day 1, suggesting fate conversion from mesoendoderm into cardiac mesoderm. The successful induction of cardiomyocytes was confirmed by both IF, showing positive staining for cardiomyocytes marker, cTNT and α-actinin (Fig. 2C), and flow cytometry, showing that around 85% of the induced cardiomyocytes express the cardiac sarcomere proteins, cTNT on day 21 (Fig. 2D).

BMP, RA and FGF signaling pathways contribute differently to the differentiation of cardiomyocytes toward SAN-like cells

Although it is generally agreed that ventricular, atrial and SAN-like cardiomyocytes are derived from different progenitor cells emerging as early as mesoderm stage, and different signaling pathways contribute differently to the directional differentiation toward ventricular, atrial and SAN-like cardiomyocytes, the timing of manipulation of the signaling pathways remains controversial. To determine the timing of manipulation, we evaluated the temporal expression of cardiac mesoderm marker (MESP1), cardiac progenitor marker (NKX2-5) and pan-cardiomyoyte marker (TNNT2) by qRT-PCR. As shown in Fig. 3, with the progression of cardiomyocyte differentiation the expression of MESP1 reached the highest level on day 5 and sharply dropped on day 7 and 10, whereas both NKX2-5 and TNNT2 were up-regulated in a time-dependent manner (Fig. 3A). These results suggest that the best time to manipulate the differentiation process is at day 5, equivalent to the cardiac mesoderm stage.

BMP4 has been shown to increase the proportion of SANLC from hiPSC. To optimize the concentration of BMP4 on the differentiation of hiPSC to the SANLPC, hiPSC was stimulated with different concentrations of BMP4 for 2 days and the expression of SAN markers, TBX18, SHOX2 and TBX3 were analyzed. Consistent with a previous report that lower concentration of BMP4 could increase the proportion of SANLPC from hiPSC, BMP4 at 1.25 ng/ml maximumly increased the expression of the SAN markers, TBX18, SHOX2 and TBX3, but not the pan-cardiomyocyte marker, TNNT2 that showed no response at lower concentrations and reached statistical significance only at 5 ng/ml. Interestingly, further increase

the concentrations of BMP4 tends to dose-dependently weaken the induction effect of BMP4 on the expression of TBX18, SHOX2 and TBX3 (Fig. 3B).

NKX2-5-mediated FGF signaling has been proposed to contribute to the differentiation of hiPSC to ventricular cardiomyocytes. To optimize the inhibition of FGF signaling pathway on the SANLPC generation, FGF inhibitor (PD) was added in the hiPSC and the expression of TBX18, HCN4, NCX2-5, and TNNT2 were analyzed. The result showed that PD dose-dependently up-regulated the SANLPC markers, TBX18 and HCN4, and down-regulated the expression of NKX2-5. As to TNNT2, PD at 450 nM significantly up-regulated its expression, which was dose-dependently inhibited by higher concentrations of PD (Fig. 3C). Taken together, PD at 960 nM is optimal.

Finally, the effect of RA signaling on SANLPC differentiation was also investigated. Treatment of hiPSC with 1 μM RA signaling inhibitor, BMS significantly increased the expression of the markers of pacemaker cells, SHOX2, TBX3 and HCN4, and of pan-cardiomyocyte marker, TNNT2 (Fig. 3D).

Combined modulation of the three signaling pathways synergistically promoted the differentiation of hiPSC to SANLC

Having optimized the conditions of manipulating BMP, FGF, and RA signaling pathways individually on the differentiation of hiPSC to SANLC, we tested whether combined usage of the three modulators BMP4 (B), PD (P), and BMS (M) has any synergistical effect. As shown in Fig. 4, BM, PM, and BPM combinations all significantly increased the expression of the markers of pacemaker cells, SHOX2, TRX3 and HCN4, and of pan-cardiomyocyte marker TNNT2 compared to those of the GiWi protocol, with the three-combination having the best induction efficiency (Fig. 4).

The BPM induction protocol leads to biased differentiation of hiPS to SANLC.

Since the BPM induction protocol significantly increased the gene expression of the markers of pacemaker cells, we next evaluated the expression of the aforementioned markers at protein level using IF and flow cytometry. IF results showed that most nuclei are positive for transcription factors, SHOX2, TBX3 and TBX18 (Fig. 5A-C). In agreement, flow cytometry data showed that BPM induction protocol generated a higher percentage of SANLC (defined by $cTNT^{+}/NKX2.5^{-}$) (55.1 ± 5%) compared to the traditional GiWi induction protocol (34.1 ± 2%) (Fig. 5D). When SANLC was defined by $cTNT^{+}/ SHOX2^{+}$, BPM protocol again generated a higher percentage of SANLC (44.5 ± 2% in the BPM versus 22.4 ± 5% in the GiWi) (Fig. 5E).

SANLC generated by the BPM protocol displays the typical electrophysiological characteristics of pacemaker cells

To evaluate the automaticity of the SANLC, cells were observed under microscopy and the beating rate was recorded. The beating rate of SANLC was significantly higher in the BPM protocol than the GiWi protocol (Fig. 6A). Since hyperpolarization-activated cyclic nucleotide-gated channel (HCN4) contributes

the most to the automaticity in SAN, inhibition of the HCN4 would decrease the automaticity of the SANLC. Consistent with our prediction, inhibition of the HCN4 using Zatebradine hydrochloride significantly decreased the beating rate of SANLC from the BPM protocol than the GiWi protocol, suggesting a higher percentage of SANLC in the BPM protocol than the GiWi protocol (Fig. 6B). We then analyzed the AP using whole cell patch clamp technique 60 days after the differentiation. Based on the morphology of AP, ratio of AP duration at 90% repolarization (APD90) to APD50, upstroke velocity and maximum diastolic potential, SANLC from both groups contain ventricle-like, atrial-like, and pacemaker-like cells (Fig. 6C). However, the percentage of pacemaker-like cells was significantly higher in the BPM protocol than the GiWi protocol (Fig. 6C).

Discussion

In this study, using the system of cardiomyocytes differentiation from hPSC by temporal manipulating the canonical Wnt signaling pathway as a model to simulate cardiac development, we discovered that SANLCs can be significantly enriched by simultaneous manipulation of BMP, FGF and RA signaling pathways. These biasedly enriched SANLCs express SAN-specific markers, are sensitive to HCN4 channel blocker, and possess the electrophysiological property of native SAN cardiomyocytes.

Biased differentiation of cardiomyocytes to SANLCs could be achieved by either manipulating the expression of SAN-specific transcription factors or using pathway-specific activators/inhibitors. For example, TBX18 is restrictedly expressed in SAN where it promotes the development of pacemaker cardiomyocytes and at the same time prevents the activation of genes leading to chamber cardiomyocyte development. Accordingly, forced expression of TBX18 in hiPSC resulted in increased differentiation to SAN-like cardiomyocytes [21]. In addition, over-expresson of TBX18 could convert the human working cardiomyocytes, adult rat bone mesenchymal stem cell and adipose derived stem cells into functional SAN-like cardiomyocytes [22, 23]. However, these methods of genetic manipulation for SAN regeneration are not desirable in future clinical applications.

Previous investigations have demonstrated that SAN like cells could be induced from different cell types by gene modification dependent strategy. In our study, we established a gene-free and chemical induced method for highly efficient differentiation of SAN like cells from hiPSC, which is more amendable in future clinical use. In a recent study, Protze S I, et al introduced a gene-free method for SAN cells induction from hPSC [24]. Based on the system of embryonic body-based cardiomyocytes differentiation, they showed that modulating the BMP and RA signaling pathway enabled highly efficient NKX25-/cTNT + SAN cells induction (55 ± 5%) indicated by flow cytometry results which is similar to our results (55.1 ± 5%). It suggested that transgene-independent method may serve as a faster, simpler and higher efficient strategy for SAN cells generation.

BMP signaling has been reported to participate in the induction of cardiac mesoderm and formation of the first heart field [17, 25]. Low concentration of recombinant BMP4 could induce cardiac mesoderm specification from hPSC and more importantly, increased the proportion of SAN-like progenitor cells in a

time window and in a dosage sensitive manner [8]. In agreement, our investigation showed that treatment of hiPSC with low concentration of BMP4 during the cardiac mesodermal stage increases the yields of SAN-like cardiomyocytes. However, increasing the dosage of BMP4 weakens the induced expression of SAN-specific markers.

FGF signaling is indispensable for promoting and maintaining the characteristics of ventricle during the early stage of heart development. Activation of FGF signaling sustains ventricular development in the early stage by maintaining the number of and the electrical characteristics of ventricular cardiomyocytes, while inhibition of FGF signaling results in a gradual accumulation of atrial cardiomyocytes, and a concomitant decreasing number of ventricular cardiomyocytes [26]. Further studies showed that NKX2-5 was the downstream regulator of the FGF signaling [13, 14]. Indeed, our study found that inhibition of FGF signaling downregulated the expression of ventricle specific makers including NKX25, while enhanced the expression of SAN makers.

RA signaling is not only essential for normal heart development but also involved in the differentiation and specification of atrial cardiomyocytes. Previous studies have shown that activation of RA signaling in hPSC differentiation is sufficient to generate cardiomyocytes displaying both electrophysiological characteristics and gene expression profile of atrial cardiomyocytes. However, study by Protze, et al. showed that activation of RA signaling increases the expression of some markers of SAN, and does not affect the induction efficiency in hPSC differentiation [24]. Our study showed that antagonizing RA signaling significantly increased the expression of SAN-specific markers SHOX2, TBX3 and HCN4 that promoted SAN differentiation. Considering the discovery by Protze, et al. that timely activation of, and the optimal activation of RA signaling promotes the maturation of SAN, we tend to believe that the biological effect of RA signaling is not just involved in atrial development but also in SAN differentiation although much more details remains to be clarified. It is worth noting that the effect of RA in the SAN development may be in the spatiotemporal dependent manner. In fact, Protze, et al. showed that the effective time window of RA treatment enhancing pacemaker characteristics is 3–7 days in the hPSC differentiation [24].

Conclusion

In summary, we have used a developmental-biology-guided approach to establish a transgene-independent highly efficient differentiation protocol for generating SAN-like cardiomyocytes from hPSC. We find that activation of BMP signaling and simultaneous inhibitions of both RA and FGF pathways during cardiac mesoderm stage of hiPSC differentiation lead to a SAN-specific gene expression landscape favoring pacemaker cell specification (Fig. 7). This provides a rich source of SAN cardiomyocytes to further study its biology and the potential applications in the treatment of arrthymia-related disease.

Abbreviations

Pluripotent stem cells, PSC, human induced pluripotent stem cell, hiPSC, sinoatrial, SA, sinoatrial node-like cells, SANLC, Sick sinus syndrome, SSS, bone morphogenetic protein, BMP, fibroblast growth factor, FGF, retinoic acid, RA, Immunofluorescence, IF, action potential, AP, GSK3 inhibitor and Wnt inhibitor, GiWi.

Declarations

Acknowledgements

N/A

Author contributions

Guarantor of integrity of entire study: Rui Zhou and Bin Liao. Study concepts: Feng Liu, Rui Zhou, and Bin Liao. Study design: Linli Wang, Rui Zhou, and Bin Liao. Literature research: Feng Liu, Xiaojie Hou, and Yibing Fang. Experimental studies: Feng Liu, Yibing Fang, Xiaojie Hou, Ying Yan, Haiying Xiao, Dongchuan Zuo and Jing Wen. Data acquisition: Feng Liu and Yibing Fang. Data analysis/interpretation: Xiaojie Hou and Ying Yan. Statistical analysis: Ying Yan and Yibing Fang. Manuscript preparation: Feng Liu, Xiaojie Hou, and Rui Zhou. Manuscript editing: Xitong Dang and Linli Wang. Manuscript revision/review: Xitong Dang and Rui Zhou. Manuscript final version approval: Rui Zhou and Bin Liao.

Funding

This work was supported by grants from the collaborative innovation center for prevention and treatment of cardiovascular disease of Sichuan province [xtcx-2019-02 to B. L., xtcx-2016-18 to R. Z.].

Availability of data and materials

The datasets used and/or analyzed during the current study are available from the corresponding author on reasonable request.

Ethics approval and consent to participate

Not applicable

Consent for publication

Not applicable

Competing interests

The authors declare that they have no competing interests.

References

1. Li R. Gene- and cell-based bio-artificial pacemaker: what basic and translational lessons have we learned? Gene Ther. 2012;19:588-95.
2. Jung JJ, Husse B, Rimmbach C, Krebs S, Stieber J, Steinhoff G, et al. Programming and isolation of highly pure physiologically and pharmacologically functional sinus-nodal bodies from pluripotent stem cells. Stem Cell Reports. 2014;2:592-605.
3. Später D, Abramczuk MK, Buac K, Zangi L, Stachel MW, Clarke J, et al. A HCN4+ cardiomyogenic progenitor derived from the first heart field and human pluripotent stem cells. Nat Cell Biol. 2013;15:1098-106.
4. Lescroart F, Chabab S, Lin X, Rulands S, Paulissen C, Rodolosse A, et al. Early lineage restriction in temporally distinct populations of Mesp1 progenitors during mammalian heart development. Nat Cell Biol. 2014;16:829-40.
5. Später D, Hansson E, Zangi L, Chien K. How to make a cardiomyocyte. 2014;141:4418-31.
6. Ma J, Guo L, Fiene SJ, Anson BD, Thomson JA, Kamp TJ, et al. High purity human-induced pluripotent stem cell-derived cardiomyocytes: electrophysiological properties of action potentials and ionic currents. Am J Physiol Heart Circ Physiol. 2011;301:H2006-17.
7. Blazeski A, Zhu R, Hunter DW, Weinberg SH, Boheler KR, Zambidis ET, Tung L. Electrophysiological and contractile function of cardiomyocytes derived from human embryonic stem cells. Prog Biophys Mol Biol. 2012;110:178-95.
8. Lee J, Protze S, Laksman Z, Backx P, Keller G. Human Pluripotent Stem Cell-Derived Atrial and Ventricular Cardiomyocytes Develop from Distinct Mesoderm Populations. Cell Stem Cell. 2017;21:179-94.
9. Zhang Q, Jiang J, Han P, Yuan Q, Zhang J, Zhang X, et al. Direct differentiation of atrial and ventricular myocytes from human embryonic stem cells by alternating retinoid signals. Cell Res. 2011;21:579-87.
10. Mommersteeg MT, Hoogaars WM, Prall OW, de Gier-de Vries C, Wiese C, Clout DE, et al. Molecular pathway for the localized formation of the sinoatrial node. Circ Res. 2007;100:354-62.
11. Mommersteeg MT1, Domínguez JN, Wiese C, Norden J, de Gier-de Vries C, Burch JB, et al. The sinus venosus progenitors separate and diversify from the first and second heart fields early in development. Cardiovasc Res. 2010;87:92-101.
12. Wiese C, Grieskamp T, Airik R, Mommersteeg MT, Gardiwal A, de Gier-de Vries C, et al. Formation of the sinus node head and differentiation of sinus node myocardium are independently regulated by Tbx18 and Tbx3. Circ Res. 2009;104:388-97.
13. Targoff KL, Colombo S, George V, Schell T, Kim SH, Solnica-Krezel L, Yelon D. Nkx genes are essential for maintenance of ventricular identity. Development. 2013;140:4203-13.
14. George V, Colombo S, Targoff K. An early requirement for nkx2.5 ensures the first and second heart field ventricular identity and cardiac function into adulthood. Dev Biol. 2015;400:10-22.
15. Targoff K, Schell T, Yelon D. Nkx genes regulate heart tube extension and exert differential effects on ventricular and atrial cell number. Dev Biol. 2008;322:314-21.

16. Dorn T, Goedel A, Lam J, et al. Direct nkx2-5 transcriptional repression of isl1 controls cardiomyocyte subtype identity. Stem Cells. 2015;33:1113-29.
17. Klaus A, Saga Y, Taketo M, Tzahor E, Birchmeier W. Distinct roles of Wnt/beta-catenin and Bmp signaling during early cardiogenesis. Proc Natl Acad Sci USA. 2007;104:18531-6.
18. Witty AD, Mihic A, Tam RY, Fisher SA, Mikryukov A, Shoichet MS, et al. Generation of the epicardial lineage from human pluripotent stem cells. Nat Biotechnol. 2014;32:1026-35.
19. Lian X, Zhang J, Azarin SM, Zhu K, Hazeltine LB, Bao X, et al. Directed cardiomyocyte differentiation from human pluripotent stem cells by modulating Wnt/β-catenin signaling under fully defined conditions. Nat Protoc. 2013;8:162-75.
20. El-Battrawy I, Zhao Z, Lan H, Cyganek L, Tombers C, Li X, et al. Electrical dysfunctions in human-induced pluripotent stem cell-derived cardiomyocytes from a patient with an arrhythmogenic right ventricular cardiomyopathy. Europace. 2018;20:46-56.
21. Gorabi AM, Hajighasemi S, Tafti HA, Atashi A, Soleimani M, Aghdami N,et al. TBX18 transcription factor overexpression in human-induced pluripotent stem cells increases their differentiation into pacemaker-like cells. J Cell Physiol. 2019;234:1534-46.
22. Kapoor N, Liang W, Marbán E, Cho H. Direct conversion of quiescent cardiomyocytes to pacemaker cells by expression of Tbx18. Nat Biotechnol. 2013;31:54-62.
23. Yang M, Zhang GG, Wang T, Wang X, Tang YH, Huang H, et al. TBX18 gene induces adipose-derived stem cells to differentiate into pacemaker-like cells in the myocardial microenvironment. Int J Mol Med. 2016;38:1403-10.
24. Protze SI, Liu J, Nussinovitch U, Ohana L, Backx PH, Gepstein L, et al. Sinoatrial node cardiomyocytes derived from human pluripotent cells function as a biological pacemaker. Nat Biotechnol. 2017;35:56-68.
25. Yang L1, Soonpaa MH, Adler ED, Roepke TK, Kattman SJ, Kennedy M, et al. Human cardiovascular progenitor cells develop from a KDR+ embryonic-stem-cell-derived population. Nature. 2008;453:524-8.
26. Pradhan A, Zeng XI, Sidhwani P, Marques SR, George V, Targoff KL, et al. FGF signaling enforces cardiac chamber identity in the developing ventricle. Development. 2017;144:1328-38.

Table

Table1. Primer sets for qRT-PCR analysis.

Gene	Direction	Sequence (5’-3’)	Product size (bp)
NANOG	Forward	TTTGTGGGCCTGAAGAAAACT	91
	Reverse	AGGGCTGTCCTGAATAAGCAG	
SOX2	Forward	GCCGAGTGGAAACTTTTGTCG	145
	Reverse	GGCAGCGTGTACTTATCCTTCT	
OCT4	Forward	CTGGGTTGATCCTCGGACCT	121
	Reverse	CCATCGGAGTTGCTCTCCA	
BRACHYURY	Forward	CAGTGGCAGTCTCAGGTTAAGAAGGA	122
	Reverse	CGCTACTGCAGGTGTGAGCAA	
MESP1	Forward	AGCCCAAGTGACAAGGGACAACT	82
	Reverse	AAGGAACCACTTCGAAGGTGCTGA	
NKX2-5	Forward	CAAGTGTGCGTCTGCCTTT	190
	Reverse	CAGCTCTTTCTTTTCGGCTCTA	
TNNT2	Forward	TTCACCAAAGATCTGCTCCTCGCT	111
	Reverse	TTATTACTGGTGTGGAGTGGGTGTGG	
SHOX2	Forward	CAAAGAGGATGCGAAAGGGAT	122
	Reverse	AGTGGGTCTCGTCAAAAAGCC	
TBX18	Forward	GACGATCTTTCTCCCATCAAGC	124
	Reverse	CTATCTTCAGGCGAGTAATCTGC	
TBX3	Forward	CCCGGTTCCACATTGTAAGAG	104
	Reverse	GTATGCAGTCACAGCGATGAAT	
HCN4	Forward	TGGACACCGCTATCAAAGTGG	157
	Reverse	CTGCCGAACATCCTTAGGGA	

Figures

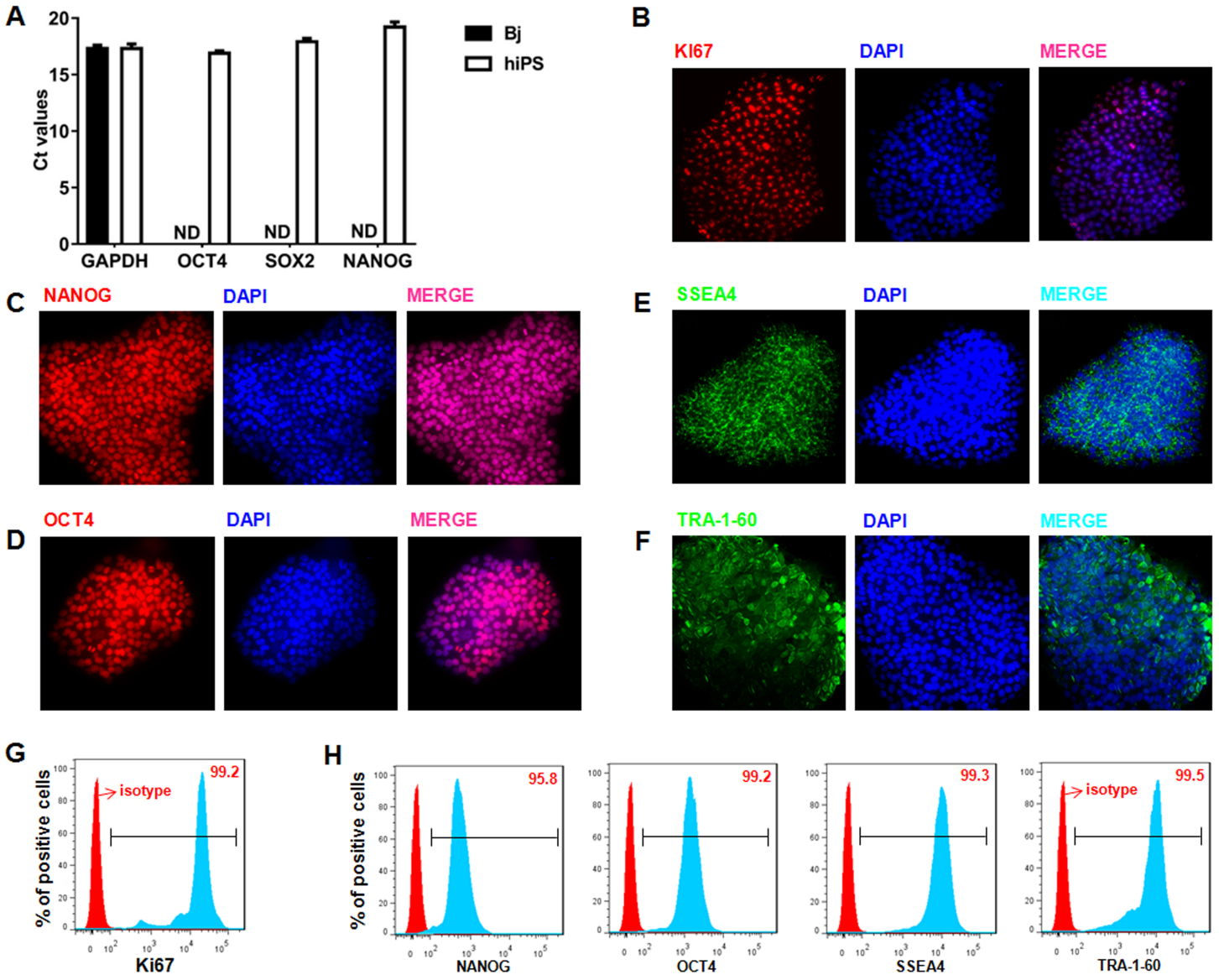

Figure 1

Characterization of the hiPSC. (A) hiPSC expresses similar high levels of the pluoripotency marker genes, OCT3/4, SOX2 and NANOG, which were comparable to the level of GAPDH gene. (B) Ki67, Pluoripotency markers of hiPSC was identified using IF method. (C-E) Pluoripotency markers of hiPSC (NANOG, OCT4, SSEA4 and TRA-1-60) were confirmed by immunoflorescence (IF) assay. (G, H) Flow cytometry analysis was further used to confirm the pluoripotency of the hiPSC. Data are presented as 'Mean ± SD'.

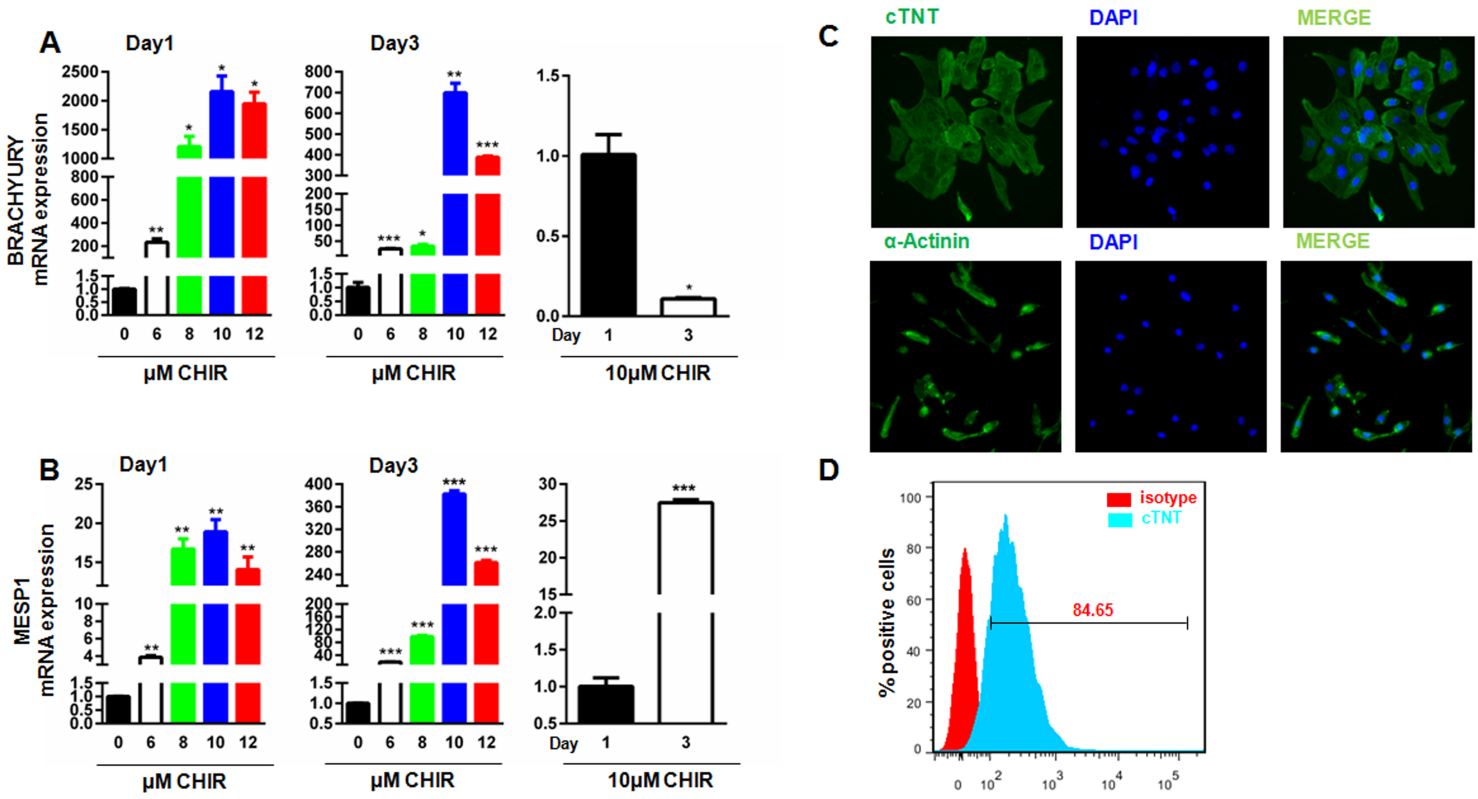

Figure 2

Characterization of the hiPSC derived cardiomyocytes. CHIR dose-dependently increased the expression of BRACHYURY(A) and MESP1(B). (C) The hiPSC-induced cardiomyocytes express cTNT and α-actinin indicated by IF assay. (D) Representative plots of flow cytometry displaying high yields of cardiomyoctes derived from hiPSC. Data are presented as 'Mean ± SD' with * denotes p <0.05, ** p <0.01, and *** p <0.001.

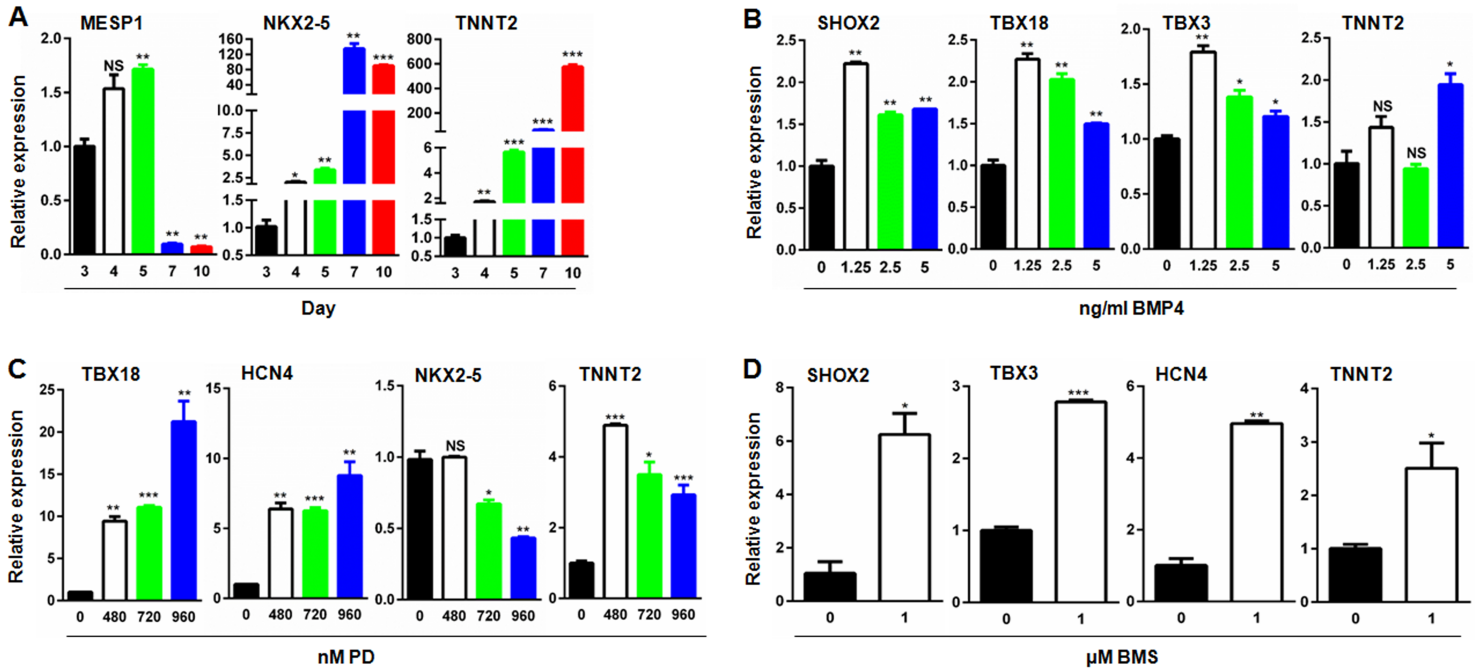

Figure 3

Optimization of the timing and dosages of small molecule chemicals targeting FGF, RA and BMP signaling pathways for enriched SANLC differentiation. (A) The expression of cardiac mesoderm marker (MESP1), cardiac progenitor marker (NKX2-5) and cardiomyoyte marker (TNNT2) on day 3, 4, 5, 7, and 10 respectively by qRT-PCR. (B) The expression of SHOX2, TBX18, TBX3 and TNNT2 was evaluated by qRT-PCR on day 16 after the differentiation of hiPSC-induced cardiomyocytes was treated with BMP4 at the indicated concentrations on day 5-7. (C) The expression of TBX18, HCN4, NKX2.5 and TNNT2 was analyzed by qRT-PCR on day 16 of the differentiation after the induced cadiomyocytes were treated with PD at the indicated concentrations on day 5-7. (D) The expression of SHOX2, HCN4, TBX3 and TNNT2 was analyzed by qRT-PCR on day 16 of the differentiation after the induced cardiomyocytes were treated with BMS at the indicated concentrations on day 5-7. Data are presented as 'Mean ± SD' with * denoting p <0.05, ** p <0.01 *** p <0.001 and NS not significant.

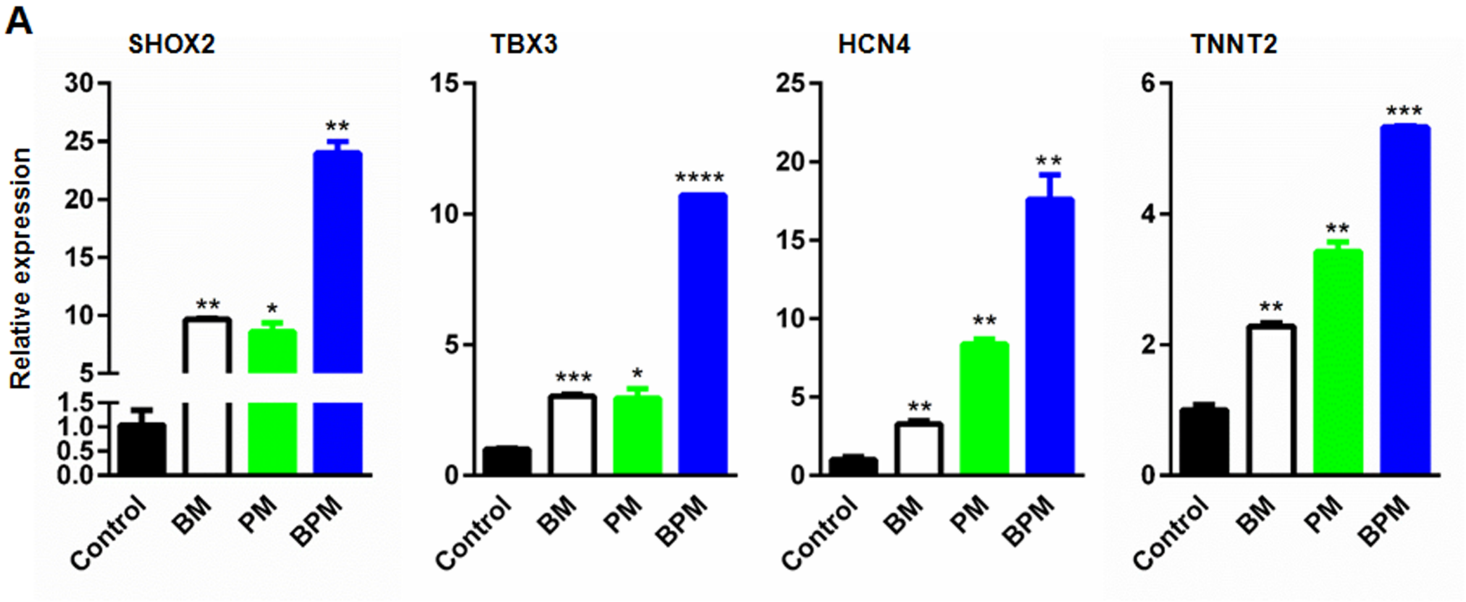

Figure 4

The BPM method promotes the differentiation of hiPSC toward SANLC. The levels of the expression of SHOX2, HCN4, TBX3 and TNNT2 (from left to right) were significantly higher in the BPM triple than BM and PM combinations Data are presented as 'Mean ± SD' with * denoting p <0.05, ** p <0.01 *** p <0.001 and **** p <0.0001.

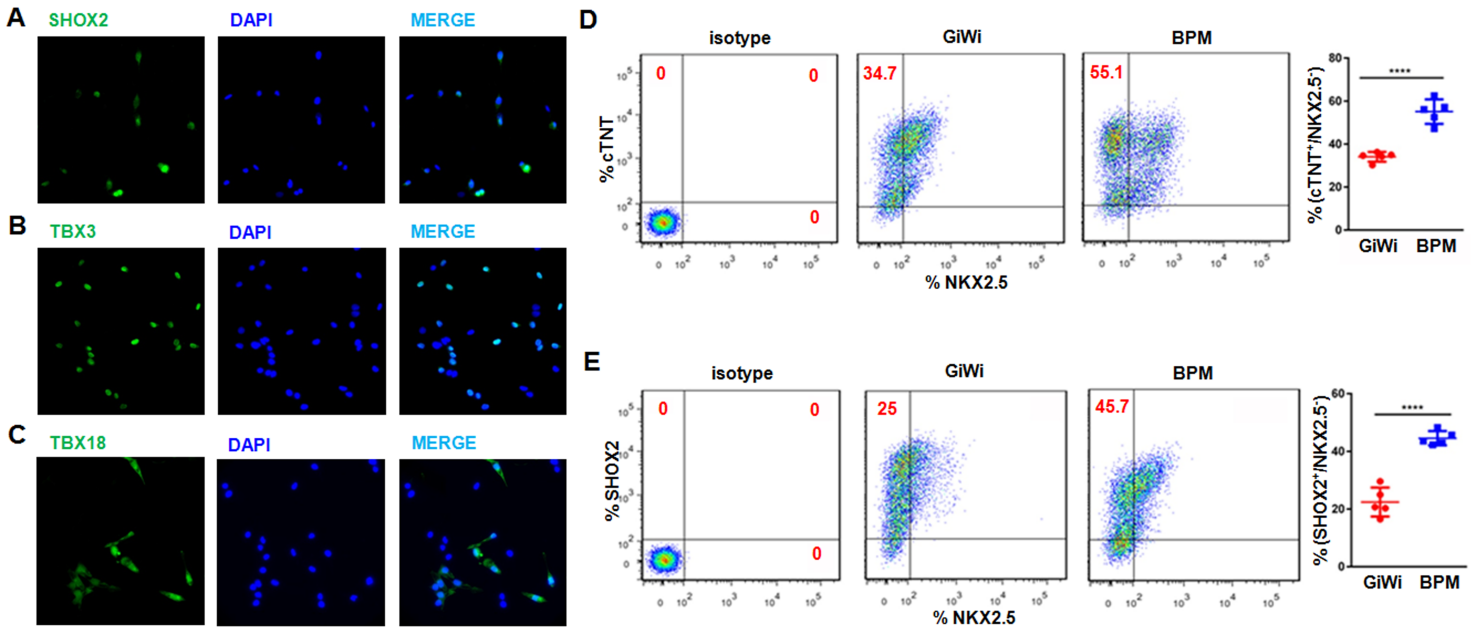

Figure 5

Validation of the enriched differentiation of SANLC by the BPM. (A-C) IF showing that SANLCs express SAN-specific transcription factor, SHOX2, TBX3 and TBX18. (D) Flow cytometry analysis showing that BPM significantly increased the percentage of CTNT+/NKX2.5- cells compared to the GiWi group (n=5). (E) Flow cytometry analysis showed that BPM significantly increased the percentage of CTNT+/SHOX2+ cells compared to the GiWi group (n=5). Data are presented as 'Mean ± SD' with * denoting $p < 0.05$.

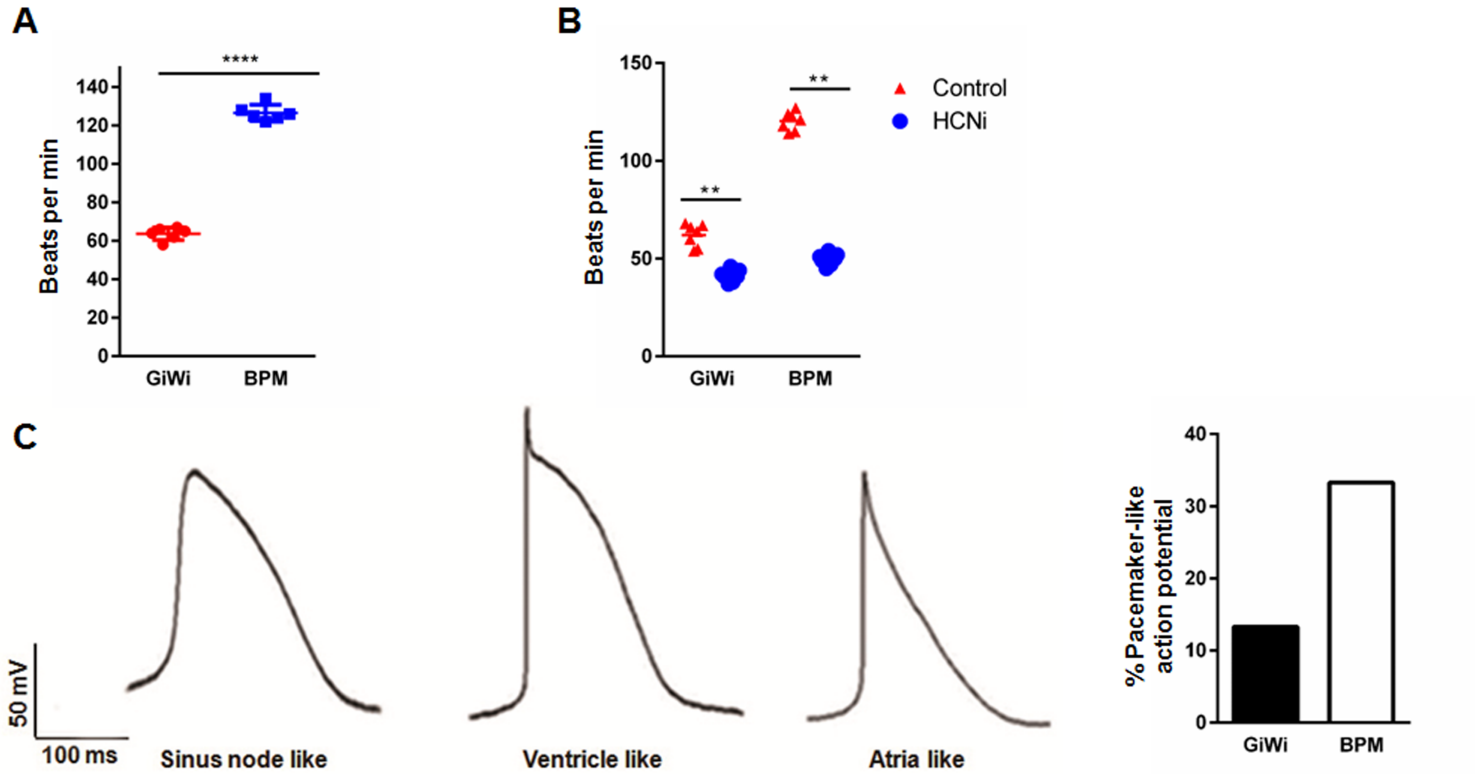

Figure 6

SANLCs induced by the BPM possess typical electrophysiological characteristics of SAN. (A) Spontaneous beating frequency of SANLCs was significantly higher in the BPM than the GiWi groups (n = 3). (B) HCN4 channel inhibitor treatment caused significantly decreased beating rate in the BPM compared to the GiWi groups. (C) Representative ventricule-like, atria-like, and sinus node-like action potential (AP) curves were recorded by whole cell patch clamp (left panel). The percentage of cells with pacemaker-like AP was remarkably increased in the BPM (n=) compared to the GiWi group (n=) (6/18 vs 2/15, BPM vs GiWi). Data are presented as 'Mean ± SD', with **** denoting p<0.0001.

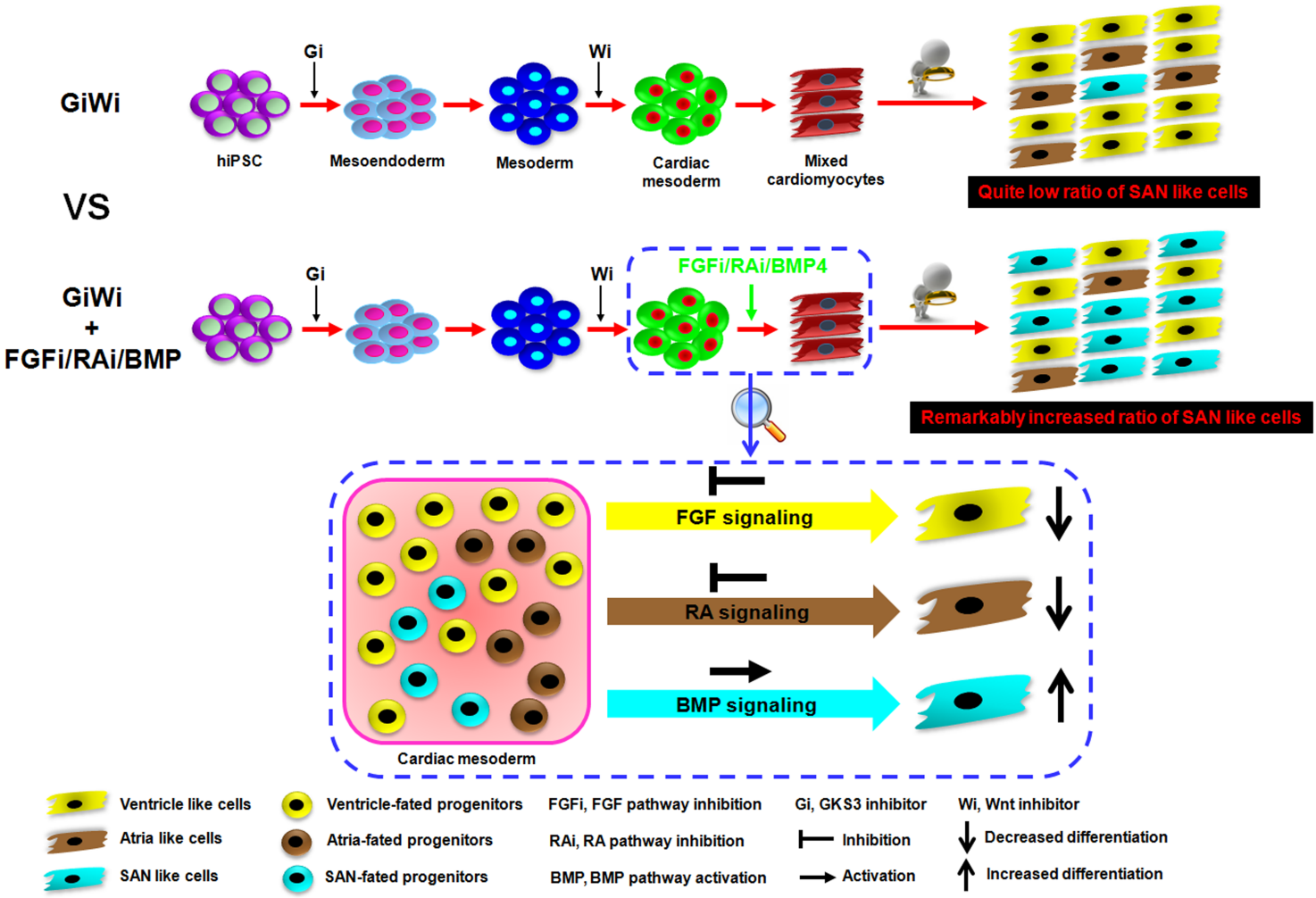

Figure 7

Graphic abstract. Working model of enriched differentiation of SANLC from hiPSC by the BPM versus the GiWi methods. Simultaneous activation of BMP and inhibition of RA and FGF signaling pathways during cardiac mesoderm stage of the GiWi-induced hiPSC differentiation strongly favors a SAN-specific gene transcriptional landscape leading to enhanced pacemaker cell specification.